Gomes-Junior, Francisco Guilhien; Moure Cicero, Silvio;
Vaz, Carlos Manoel Pedro; Orlandi Lasso, Paulo Renato
X-ray microtomography in comparison to radiographic analysis of
mechanically damaged maize seeds and its effect on seed germination

X-ray microtomography in comparison to radiographic analysis of mechanically damaged maize seeds and its effect on seed germination

Francisco Guilhien Gomes-Junior[1]* , **Silvio Moure Cicero[1]**, **Carlos Manoel Pedro Vaz[2]** and **Paulo Renato Orlandi Lasso[2]**

[1]Departamento de Produção Vegetal, Escola Superior de Agricultura "Luiz de Queiroz", Universidade de São Paulo, Av, Pádua Dias, 11, Cx. Postal 09, 13418-900, Piracicaba, São Paulo, Brazil. [2]Empresa Brasileira de Pesquisa Agropecuária, Embrapa Instrumentação, São Carlos, São Paulo, Brazil. *Author for correspondence. E-mail: francisco1@usp.br

ABSTRACT. Among the most relevant aspects of seed production, mechanical damage may affect seed germination and reduce health and vigor. This study introduces a noninvasive high-resolution imaging procedure for evaluating the mechanical damage to maize seeds and the effects on seed germination. Seeds with different levels of mechanical damage were evaluated using a benchtop micro-computed tomography system (micro-CT) and digital X-ray equipment. The two-dimensional transaxial, coronal and sagittal micro-CT sections were used to inspect the seed anatomy and the mechanical injuries in the internal seed tissue. Germination tests were performed using paper towel rolls (25°C for 7 days) in which the seedling length was evaluated on a daily basis, and the seedling dry biomass was measured at the seventh germination day. The micro-CT cross-sectional images allowed an efficient spatial characterization of the mechanical damage inside the seeds. On average, mechanically damaged seeds produced seedlings with a length 24% shorter and a dry biomass 65% less than that of the undamaged seeds. We concluded that the micro-CT technique provides an efficient means to inspect mechanically damaged maize seeds and allows for a reliable association with germination response.

Keywords: *Zea mays*; seed internal morphology; 3D X-ray imaging; computed tomography.

Introduction

Mechanical damage affects seed quality (Bewley & Black, 1994) along with harvesting, transporting, drying and handling (Carvalho & Nakagawa, 2012). Mechanical damage is associated with a loss in physical integrity, higher susceptibility to microorganism infection, sensitivity to chemical treatment, and decrease in physiological quality and seed lot storability (Bewley & Black, 1994).

An improvement in the evaluation of mechanically damaged maize seeds occurred in late 1990s when X-ray radiography was introduced as a non-invasive technique for analyzing internal injuries of seeds along with their physiological quality (Cicero, Heijden, Van der Burg, & Bino, 1998; Carvalho, Aelst, Eck, & Hoekstra, 1999). Research evaluating pre-harvesting cracks on maize seeds using X-ray radiography and low-temperature scanning electron microscopy showed that internal injuries or those perpendicular to the embryonic axis affect seed germination and vigor (Carvalho et al., 1999). Nevertheless, further research has shown that in some situations, radiographic analysis was not satisfactory in identifying injuries associated with the poor germination. Because radiographic analysis is a two-dimensional (2D) projection of a seed, it is not effective in determining depth of cracks. Cicero and Banzatto-Junior (2003) showed that 23% of maize seeds with mechanical damage on the embryo produced normal seedlings and concluded that the X-ray radiography technique did not allow for an accurate evaluation of fractures.

Several imaging techniques, such as magnetic resonance imaging (MRI) (Ghosh, Jayas, Gruwel, & White, 2006), synchrotron X-ray fluorescence (De Jonge & Vogt, 2010), X-ray absorption (Staedler, Masson, & Schönenberger, 2013), phase contrast (Cloetens, Mache, Schlenker, & Lerbs-Mache, 2006) and neutron tomography (Cleveland IV et al., 2008), have been applied to plant and seed analysis. Among the techniques, high-resolution desktop X-ray absorption tomography (micro-CT) is highly recommended because of its excellent contrast, which allows flexibility to analyze different biological and mineral materials and it increases commercial instrumentation availability (Stuppy, Maisano, Colbert, Rudall, & Rowe, 2003; Pittia et al., 2011; Milien, Renault-Spilmont, Cookson, Sarrazin, & Verdeil, 2012; Dawson, Francis, & Carpenter, 2014; Friis,

Marone, Pedersen, Crane, & Stampanoni, 2014). Unlike radiography, which is a projection image, micro-CT produces a pack of two-dimensional cross-sectional images that can be combined into a three-dimensional image allowing internal inspection and measurement (Stuppy et al., 2003). The objective of the present study was to establish an optimized procedure to acquire high-resolution X-ray microtomographic images of dry damaged maize seeds to evaluate their internal morphology and the damage's effect on seed germination.

Material and methods

Available equipment to induce seed damage

The seeds were mechanically damaged using the S-injure equipment (Figure 1). The equipment is a box (made of medium-density fiberboard) measuring $40 \times 25 \times 37$ cm. The seeds were thrown against a stainless-steel plate (3 mm in thickness) via a pressure regulator (Arprex, model AF1) operating up to a pressure of 828 kPa. A seed sample of 400 g was launched three times against the stainless-steel plate positioned 13 cm from the exit of the seed ejector tube with a pressure of 414 kPa, resulting in an average speed of 40 m s^{-1}. The seeds were released into a hopper and thrown against the steel plate. Subsequently, the seeds were collected in a drawer positioned at the base of the equipment, and the process was repeated two more times.
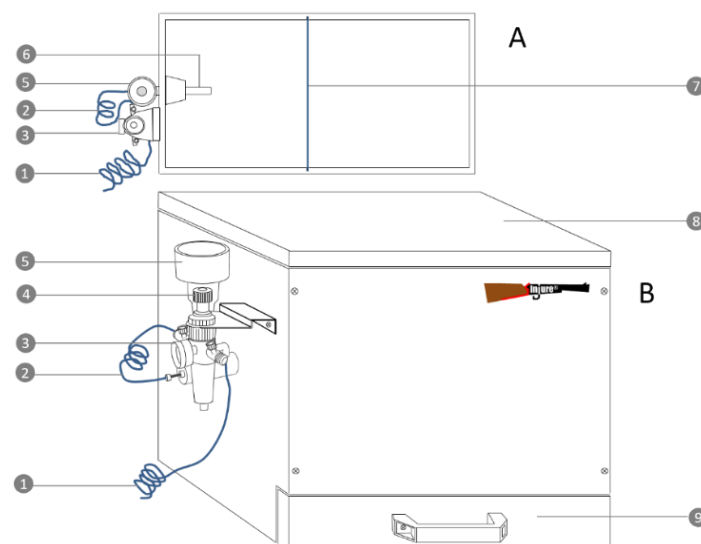

Figure 1. Schematic diagram of the S-injure equipment used to induce seed damage. Superior view (A) and 3D view (B). 1 - entrance of compressed air; 2 - controlled compressed air injection; 3 - manometer; 4 - pressure controller; 5 - seed hopper; 6 - seed ejector tube; 7 - steel plate; 8 - cover; and 9 - catch drawer.

Maize seed selection

We investigated seeds with 12% moisture content (wet basis) of the hybrid 2B604PW (flat seeds classified in sieves with oblong screens measuring 20/64" × 3/4" = 7.9 mm × 19.0 mm; 1000 seed mass = 330.29 ± 12.05 g) with greater than 95% germination. After mechanical damage was induced, a cabinet X-ray system for specimen radiography (Faxitron X-ray, model MX-20 DC12, Tucson, USA), operating from 10 to 35 kV, 300 μA and with a maximum pixel resolution of 7 μm, was employed to image and select 25 seeds of different mechanical damage levels (based on injury extension in the embryo and/or endosperm) for micro-CT image analysis and germination tests using the same set of seeds. Seeds were stored in individual and numbered plastic cell trays, and all subsequent analysis (micro-CT and germination characteristics) was registered and assigned for each individual seed.

Micro-CT parameters

Twenty-five seeds were individually scanned using a SkyScan 1172 benchtop micro-CT system (SkyScan, Belgium, actually Bruker). This equipment relies on cone beam geometry and comprises a tungsten X-ray microfocus tube with < 5-μm focal spot and a sealed, fully distortion-corrected, air-cooled, 10-Mp, 12-bit CCD camera that is fiber-optically coupled to a Gd_2O_2S scintillator. Each seed was attached on the rotating sample

stage using double-sided bounding tape, with the seed embryo facing upward. To avoid unwanted movement during scanning, Parafilm M was used to wrap and attach the seed on the sample stage (Figure 2).
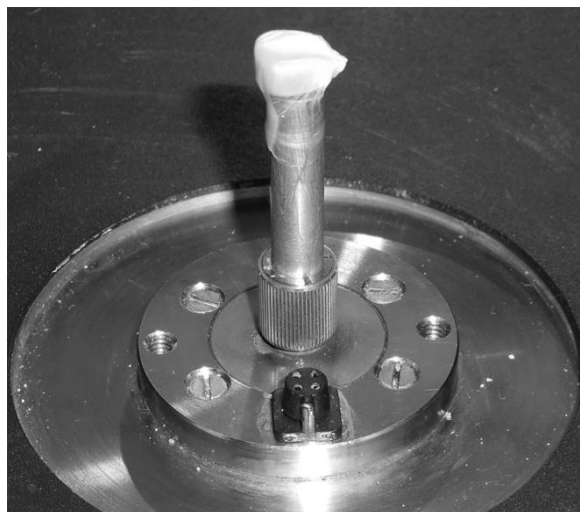

Figure 2. Image of one maize seed on the micro-CT SkyScan 1172 brass stage (5 mm in diameter) covered with Parafilm to avoid movement during image acquisition.

We evaluated the following parameters: i) camera resolutions of 2000 × 1048 pixels (2K mode) and 4000 × 2300 pixels (4K mode); ii) no filter and a metallic filter (aluminum, 0.5 mm in thickness) positioned between the camera and sample stage; iii) angular rotation steps (0.2° and 0.3°) and total rotation (180° and 360°), and with the number of shadow projections (frames) averaged in each rotation step to optimize image acquisition and reconstruction. The operational X-ray tube voltage and current were 89 kV/112 μA when applying the aluminum filter or 59 kV/167 μA without the filter. Image reconstruction was performed using the NRecon software package (http://www.skyscan.be/products/downloads.htm). For image reconstruction, we applied and optimized beam hardening, a rings artifact and a filter for noise reduction.

Evaluation of time of X-ray irradiation on seed germination

Groups of five seeds were irradiated for 0, 1, 2, 3 and 4 hours using the micro-CT system operating at 89 kV/112 μA to evaluate whether the X-ray irradiation during the scanning affected seed germination. Afterward, the seeds were weighed using an analytical precision balance (readability: 0.0001 g) and germinated in paper towel rolls (25°C for 5 days) moistened with water equivalent to 2.5 times the mass of the dry paper. Seeds were positioned on the upper third of the paper, maintaining the hilum orientation toward the paper bottom, allowing the seedling to grow straight. Germination performance was evaluated by the length and dry biomass of the seedlings. Seedling length was determined measuring the distance from the apical bud to the tip of the primary root using a graduated ruler in millimeters, and the seedling dry biomass was weighed after oven-drying at 80°C for 24h.

Seed internal morphology and damage characterization using micro-CT image analysis

Based on optimized acquisition and reconstruction parameters, intact seeds and seeds showing different levels of mechanical damage were analyzed using the micro-CT scanner. Reconstructed cross-sectional grayscale images were stored in 8-bit BMP format files. The SkyScan 1172 system was controlled using a host personal computer (dual core Xeon processor [Intel, Santa Clara, CA], 3 GHz, 4 GB RAM, 1 TB HD), and image reconstruction was performed using a 2 PC cluster (dual core Xeon processor, 3 GHz, 2 GB RAM, 500 GB HD). The reconstructed sections of each seed were analyzed using the DataViewer software (version 1.5.1.2). The two-dimensional (2D) coronal (XZ), sagittal (ZY), and trans-axial (XY) planes were used to inspect the seed anatomy and changes caused mechanical damage in internal tissue. Two coronal views (one through the endosperm, C1, and another through the endosperm + embryo, C2) were selected for quantitative seed analysis. Parameters such as cross-sectional seed area (mm^2) and percentage of damaged area were determined using ImageJ software (Schneider, Rasband, & Eliceiri, 2012). A total of 30 seeds were inspected (25 mechanically damaged and 5 undamaged), and comparative analyses were performed between micro-CT and X-ray radiography.

Seed germination and seedling vigor

We complete the seed germination tests using paper towel rolls under the same conditions of moisture and temperature, as previously described. The intact and damaged seeds (in groups of five) were positioned in the upper third of the paper and identified by their numeric codes. Seedling length was measured daily for 7 days (at 10:00 am) using a ruler. Seedling images were captured on the seventh day using a flatbed scanner (HP, model Scanjet 200) at a resolution of 600 dpi. Seedling dry biomass was also determined on the seventh germination day. The results were evaluated and discussed comparing the damaged area assessed using the micro-CT images with the seed germination parameters.

Results and discussion

Micro-CT acquisition and reconstruction parameter optimization

According to the average size of the analyzed maize seed, the spatial resolution (voxel size) was 6.5 μm, allowing complete seed visualization using the rectangular charge-coupled-device (CCD) camera. Acquisition time for collecting a complete set of projection images without the metallic filter was 75 and 140 minutes in the 2K and 4K modes, respectively. As a preliminary quality analysis of the reconstructed images indicated good contrast in internal seed parts for the micro-CT images acquired in the 2K mode, such a configuration was selected due to its shorter acquisition time. Other acquisition parameters, selected based on image contrast and signal-to-noise analysis, were five frames for each projection image, an angular rotation step of 0.2° and a total rotation of 180°, which generated approximately 900 projection images during the whole acquisition process.

Reconstructed cross-sectional images obtained when no metallic filter was employed showed considerable beam-hardening artifacts (Boas & Fleichsmann, 2012), as indicated by sharp increases in the image intensity profiles at the seed-air limits, as shown in Figure 3A, where no beam-hardening correction was applied (BH0).
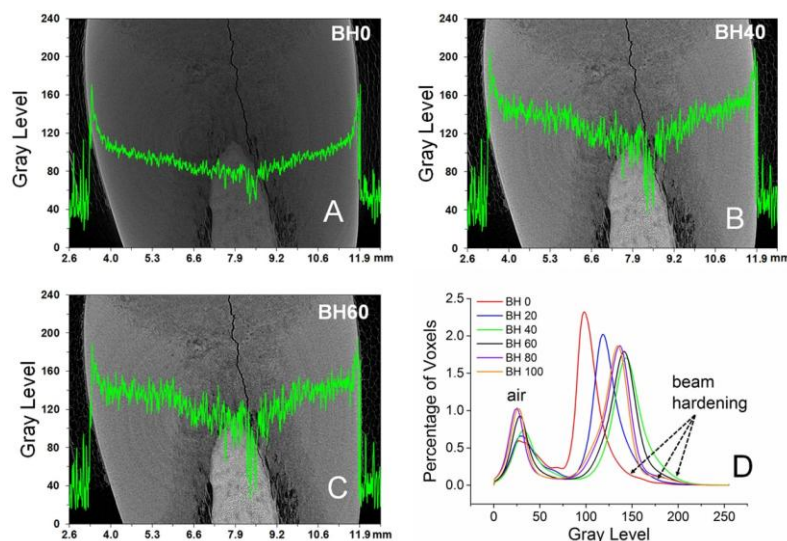

Figure 3. Reconstructed micro-CT images of a maize seed using different beam-hardening (BH) artifact correction intensity (A to C), and grayscale histograms of the entire seed image volume for BH corrections of 0, 20, 40, 60, 80, and 100%. The dotted lines indicate the gray level profile positions in A, B, and C.

However, when the aluminum filter was employed, beam hardening was, on one hand, considerably reduced, but on the other hand, the contrast among the internal parts significantly decreased. Therefore, acquisition without the use of a metallic filter was selected, and the mathematical correction provided by the NRecon software was applied to reduce beam-hardening image artifacts (Figure 3B and C). Image intensity (grayscale) histogram analysis was used to select the beam-hardening correction intensity (Figure 3D). Beam hardening can be observed using asymmetric histogram curves tailored to a higher image intensity grayscale (at gray levels between 125 and 200) for beam-hardening (BH) corrections of 0, 20 and 40%. Therefore, a correction was set to 60% (Figure 3C) for image reconstruction using the NRecon software to minimize BH effects while avoiding distortion and maintain a low signal-to-noise ratio.

Ring artifacts (concentrated superimposed rings) are among the most common image artifacts in reconstructed tomographic sections and are caused by defective or miscalibrated detector elements (Boas &

Fleischmann, 2012; Friis et al., 2014). This image artifact was only slightly present in the maize seed micro-CT images (Figures 3, 6 and 9) and had a negligible effect on the image parameters evaluated. The micro-CT images also present noise problems, which can be reduced using iterative reconstruction to smooth them out (Boas & Fleischmann, 2012). Smoothing filters for noise reduction and mathematical correction of ring artifacts were set to 2 and 20, respectively. These optimized acquisition and reconstruction parameters provided the best compromise between image quality, allowing for the visualization of the internal structures of the maize seeds and the image acquisition time. The total image reconstruction time was approximately one hour, resulting in approximately 135 minutes needed to fully process the image acquisition and reconstruction for each maize seed with an image spatial resolution of 6.5 μm.

Germination of X-ray irradiated maize seeds

Radiation doses equivalent to X-ray irradiation times up to 4 hours (approximately three times the image acquisition period for one seed) did not affect length and seedling dry biomass (Figure 4), as no reduction was observed for these parameters in comparison to those of the non-irradiated seeds (0h). Seedling length ranged from 20.8 to 26.4 cm and seedling dry biomass from 59.7 to 70.9 mg. The mass of the seeds employed during the experiment was quite uniform (330.29 ± 12.05 mg per seed) to ensure that there was no influence on the length and dry biomass of the seedlings. These results agree with previous studies using X-ray radiography on maize seed germination in which no harmful effects on seed germination were observed (Bino, Aartse, & Van der Burg, 1993; Girardin, Chavagnat, & Bockstaller, 1993; Cicero et al., 1998; Carvalho et al., 1999; Cicero & Banzatto-Junior, 2003; Gomes-Junior & Cicero, 2012).
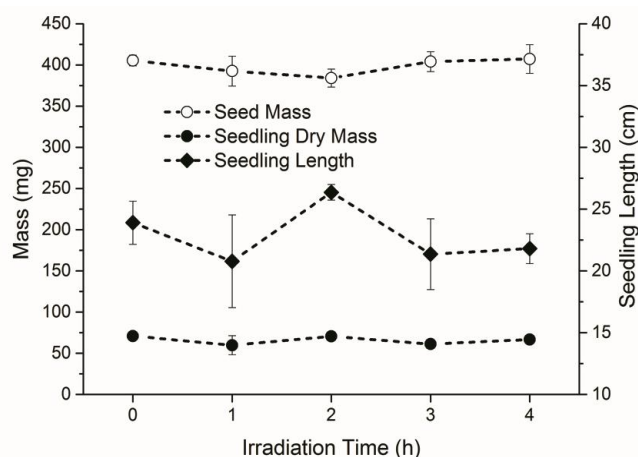

Figure 4. Effect of maize seed exposure to X-ray irradiation using the SkyScan 1172 micro-CT system on seedling length and dry biomass. Bars correspond to the standard error of the mean (set of five seeds).

According to Bino et al. (1993), low energy X-rays and short exposure times are not detrimental to cells and do not affect germination. Carvalho, Silva, Oliveira, Silva, and Caldeira (2009), studying pumpkin seeds using a 45-keV energy X-ray source and 25 seconds of irradiation time, did not identify any effects on seed germination and vigor, even after one year of storage. Furthermore, in the present research, as high-energy X-ray doses were used (89 keV), the radiation dose absorption tended to be lower, reducing the probability of negative effects on maize seed germination, although additional studies are needed to evaluate the consequences on seed physiological potential following different storage periods. Lower energy doses may result in higher levels of radiation damage as a greater amount of energy is absorbed by the seed. Research conducted on canola and wheat seeds exposed ten times to X-ray energy doses of 40 keV also showed no effects on germination (Young, Parham, Zhong, Chapman, & Reaney, 2007). These results demonstrate that experiments using high X-ray energy doses may be useful for studying seed morphological features associated with seed physiological potential, as radiation damage is avoided.

Morphological maize seed analysis suing X-ray micro-CT and radiography

Figure 5 shows radiographic projection images of an intact (S26) and three mechanically damaged (S18, S3, and S24) maize seeds and their respective seedlings on the seventh day of germination. The radiographic images allow some degree of internal seed morphology visualization, mainly to identify the scutellum, plumule, radicle and endosperm.
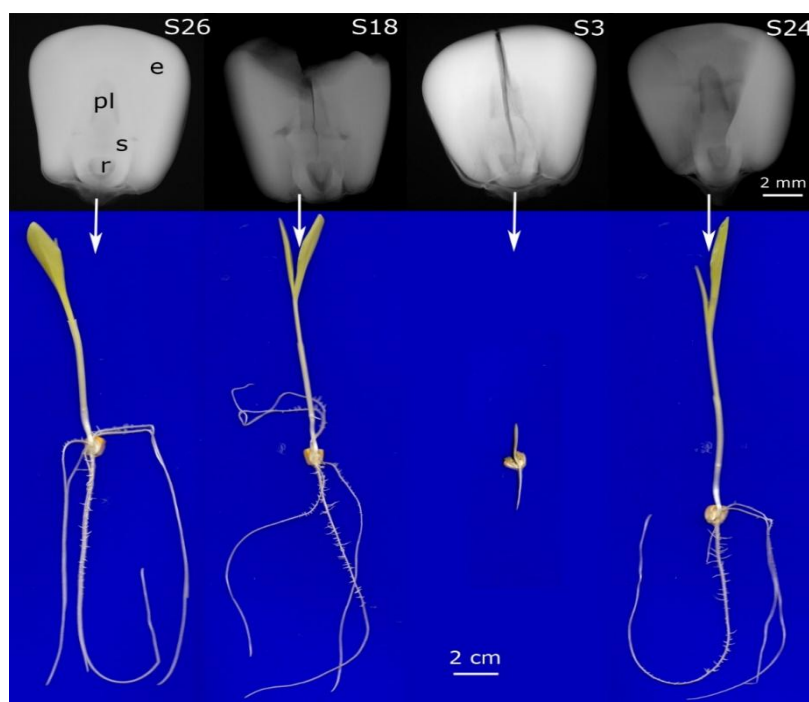
Figure 5. Radiographic images of an intact (S6) and three mechanically damaged maize seeds (S18, S3, S24) (at the top) and scanned images of their seedlings on the seventh germination day (at the bottom). Seed S3 developed an abnormal seedling. Internal parts shown in S26 are the e = endosperm, pl = plumule, r = radicle, and s = scutellum.

Overall, the undamaged seeds were easily separated from those with different levels of mechanical damage, but as projection images, radiography does not allow evaluating in-depth the real extension of cracks. Two-dimensional micro-CT images of the coronal, transaxial (transverse, axial) and sagittal planes of seeds S26 (intact), S18 and S3 (mechanically damaged) are shown in Figure 6. The red, green and blue lines indicate the coronal, sagittal and transaxial cut planes, respectively. The micro-CT images allowed much more accurate visualization of the internal seed parts (embryonic axis, scutellum, plumule, radicle and endosperm) compared to the radiographic images. Clear differences in X-ray attenuation (gray levels) were observed between the embryo (scutellum + embryonic axis) and endosperm, and different regions of the endosperm, as indicated by the red arrows in Figure 6A.

In general, the micro-CT technique was always more efficient compared to radiography in evaluating mechanical damage. The radiographic image of seed S3 shown in Figure 5 has a longitudinal fracture throughout the embryonic axis, but their cross-sectional micro-CT images (Figure 6C) depict a main fracture and several small fractures propagating through the endosperm, scutellum and scutellum boundaries (red arrows in Figure 6C). In seed S18 (Figure 6B), the mechanical damage induced small cracks in different regions of the endosperm and significant mass disruption but without reaching the embryonic axis. It is notable that for this seed (S18), the radiographic image did not show such small cracks in the endosperm but was able to detect the major damage on the endosperm and embryonic axis (Figure 5). The production of the normal seedling was only explained by the transaxial micro-CT sections through the plumule and seminal roots region and the radicle of seed S18 (Figure 6B), confirming that the embryonic axis was undamaged (which is different from what appeared in the radiographic image).

X-ray radiographic analysis has been previously applied to evaluate the mechanical damage of maize seeds (Girardin et al., 1993; Cicero et al., 1998; Carvalho et al., 1999; Cicero & Banzatto-Junior, 2003; Gomes-Junior & Cicero, 2012). One of these studies reported that the transversal ruptures in the endosperm may affect the embryonic axis and reduce the percentage of seed germination (Cicero et al., 1998). Furthermore, when injury was perpendicular to or through the embryonic axis, the result was an abnormal seedling (or seed death) in both germination and vigor (cold test) evaluations (Cicero et al., 1998; Carvalho et al., 1999; Cicero & Banzatto-Junior, 2003). In seed S3 (Figure 5), the mechanical damage through the embryonic axis affected the germination, resulting in an abnormal seedling and confirming results of previous research. However, it is important to emphasize the incipient shoot and root development indicating that the crack was not sufficiently deep to reach the embryonic axis, as it was confirmed only by the micro-CT sections (Figure 6C).

This observation confirms the limitation of the 2D X-ray imaging in identifying the real location of injuries inside a seed. Another example, as reported by Carvalho et al. (1999), was related to the crack orientation within the seed, i.e., if the crack is perpendicular to the X-ray beam, it will appear as a line and will be identified. However, if it is parallel to the X-ray beam, it will appear as a dot on the image and not be recognized as a crack.
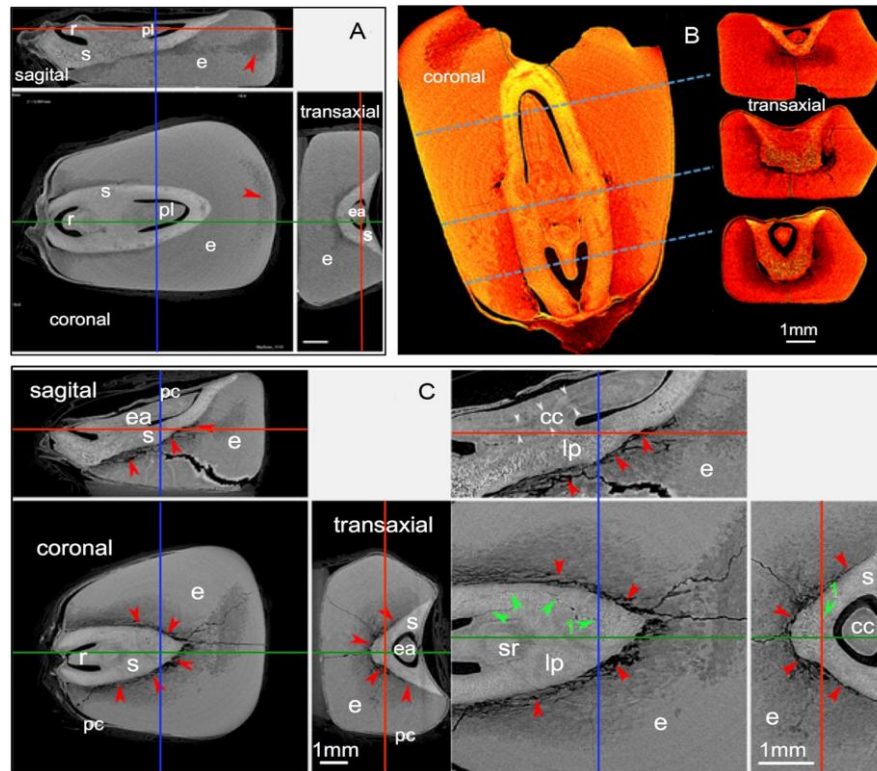

Figure 6. Coronal, sagittal and transaxial micro-CT planes of the maize seeds shown in Figure 5. Seed S26 (A) is an intact and S18 (B) and S3 (C) are mechanically damaged seeds. Arrows in seed S26 indicate less dense areas in the endosperm tissues and gray level variations are observed between the embryo and endosperm. Coronal sections of seed S18 (B) are presented for the plumule and seminal roots region and radicle. Red and green arrows in the zoomed views of seed S3 show cracks between the scutellum and endosperm and cracks on the scutellum, respectively (C). Green arrows labeled "1" (C) indicate a microfissure in the transaxial and coronal planes of seed S3. Abbreviations: cc = central cylinder, e = endosperm, ea = embryonic axis, lp = lipid granules, pc = pericarp, pl = plumule, r = radicle, s = scutellum, and sr = seminal roots region.

Germination performance of damaged and undamaged maize seeds

The effect of mechanical damage on seed germination was assessed by the seedling length and seedling dry biomass. Comparisons of seedling length from damaged and undamaged seeds are shown in Figure 7. On the second germination day (Figure 7A), the seedling length of all damaged seeds was equal to or higher than the average seedling length (dashed line) for the set of five undamaged seeds. On the fourth germination day and thereafter, the seedling length of the average mechanically damaged seeds was lower than the average undamaged seeds (dashed lines), and the difference increased with germination time (Figure 7C, D, E, and F), in which only four damaged seeds produced longer seedlings than the average undamaged seeds (S8, S11, S18, and S24). The damaged seed S18, shown in Figure 5 and Video 1, produced a 42.1-cm-long normal seedling that was 15 cm longer than the average size of the undamaged seeds (27.1 cm) on the seventh germination day. Similar mass disruption was observed in seed S24 (Figures 5 and 9), where a large portion of the endosperm was removed because of the mechanical damage. Abnormal seedlings, such as the one shown in Figure 5 for seed S3, also occurred for seeds S1, S2, S16 and S19 (Figure 7F). The abnormal seedling produced from seed S3 (Figure 5) may be attributed to poor nutrient translocation to the embryonic axis because of the cracks in the scutellum boundary, as the embryonic axis remained intact. It is important to emphasize that this mechanical damage bypassing the scutellum was only observed in the micro-CT sections, and thus this technique was decisive in explaining the poor germination.
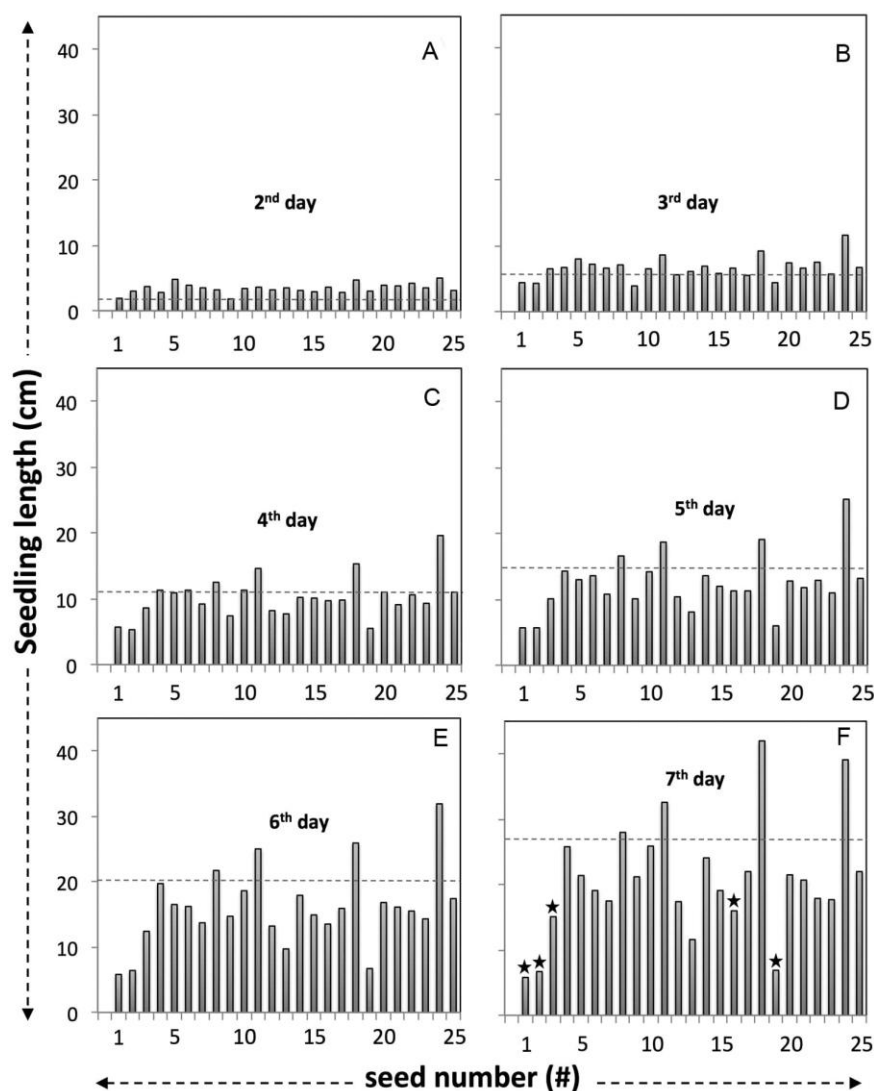
Figure 7. Seedling length of 25 mechanically damaged maize seeds under the germination test at 2, 3, 4, 5, 6 and 7 days. The dashed lines represent the average seedling length of five undamaged seeds on the different days. The stars indicate the abnormal seedlings on day 7.

In addition, micro-CT images showed small cracks or microfissures and internal structure visualization of similar resolution to that obtained by Carvalho et al. (1999) using scanning electron microscopy to evaluate internal injuries in maize seeds, but with the advantages of being a non-invasive method and not requiring sample preparation. With an image spatial resolution of 6.5 μm, micro-CT allowed evaluation of the extent and depth of cracks confirming whether the embryonic axis was affected or not, as shown in Video 1 for seed S18. Despite losing part of the endosperm, no injuries were observed along the embryonic axis and scutellum boundary, which may explain the better germination compared to that of seed S3 (abnormal seedling).

In general, the longer seedling length observed for the damaged seeds until two days of germination may be attributed to easy water access to the endosperm tissue and rapid reserve mobilization to the root and shoot meristems, as also reported by Carvalho et al. (1999). Although some damaged seeds had a longer seedling length on the seventh germination day (Figure 7F), all damaged seeds produced lighter seedling dry biomass compared to that of all the undamaged seeds (Figure 8C) and to the average seedling length as well (Figure 8D). These results confirmed the negative effects of mechanical damage on the germination and vigor of maize seeds. Furthermore, despite the lower mass of some damaged seeds losing fractions of the endosperm (Figures 8C and 9), which was also associated with highly damaged areas by micro-CT coronal views C1 and C2 (Figure 8A and B), the reduction in seedling dry biomass was similar to that of the others damaged seeds.
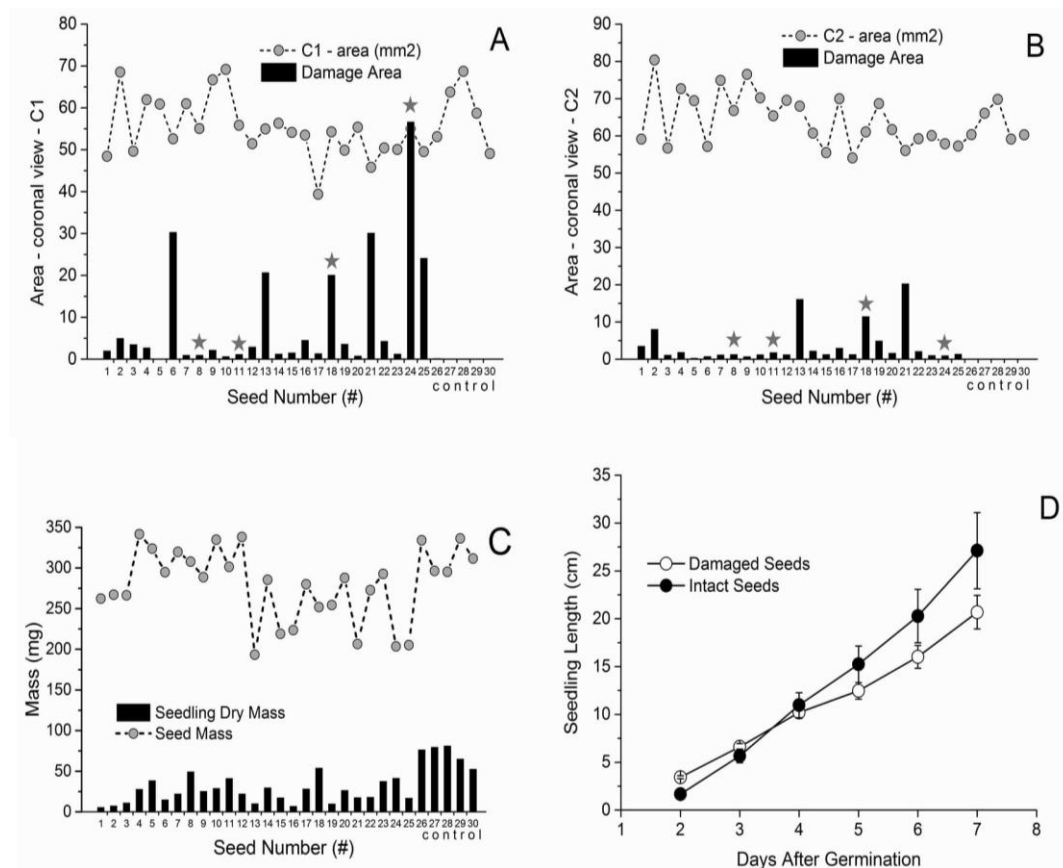
Figure 8. Seed area in the endosperm - C1 (A) and endosperm + embryo - C2 (B) micro-CT coronal views and their respective percentage of damaged area evaluated using the ImageJ software. The mass of damaged seeds (S1 to S25) and undamaged maize seeds (S26 to S30) and their respective seedling dry biomass (C). The average seedling length of the damaged and undamaged seeds from the second to the seventh germination day (D). The stars in A and B indicate damaged seeds that produced a longer seedling length compared to the average of the undamaged seeds on the seventh germination day. The bars in D correspond to the standard error of the mean.

The damaged seed areas evaluated in coronal planes C1 (endosperm) and C2 (endosperm + embryo) are shown in Figure 8A and B. The percentage of damaged area showed a large variation among seeds reaching a maximum of 57% for seed S24 in C1 and 20% for seed S21 in C2. Despite these very large damaged areas, some seeds showed longer seedling length compared to the averaged seedling length of the undamaged seeds (Figure 7: S8, S12, S18, and S24). Nevertheless, the average seedling dry biomass of the damaged seeds (S1 to S25) was lower, approximately 25 mg against 71.6 mg for the undamaged seeds (S26 to S30) (Figure 8C and Table 1), and the average dry mass of the damaged and undamaged seeds was 280.7 mg and 323.7 mg, respectively.
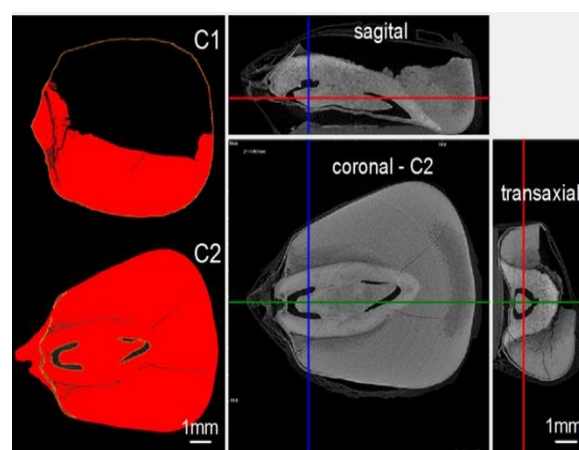

Figure 9. Endosperm (C1) and endosperm + embryo (C2) coronal planes of seed S24 processed using the ImageJ software and their sagittal coronal and transaxial micro-CT image planes. Damaged areas in C1 and C2 were 57% and 1%, respectively.

Table 1. Average values and standard deviation (STD) of some selected seed germination parameters.

Parameter	unit	MD*	UD*
N: number of seeds		25	5
sm: seed mass	mg	280.7	323.7
STD*- sm	mg	44.9	18.2
sdm: seedling dry biomass	mg	25.0	71.6
STD*- sdm	mg	13.2	10.7
sdl: seedling length	cm	20.7	27.1
STD*- sdl	cm	8.6	8.0
C1: seed area at coronal plane C1	mm^2	54.8	58.7
DA - C1: damaged area at section C1	mm^2	4.77	0.05
C2: seed area at coronal plane C2	mm^2	64.3	63.1
DA - C2: damaged area at section C2	mm^2	2.41	0.03

*STD: standard deviation; MD: mechanically damaged seeds; and UC: undamaged seeds.

Correlations between the percentages of seed damaged area measured using the micro-CT image technique in coronal planes C1 and C2 and seedling length and biomass are depicted in Figure 10. For up to approximately 10% of the damaged area, seedling length and biomass decreased drastically in both C1 and C2. Seeds with a damaged area in C1 and/or C2 greater than 10% may be identified in Figure 8A and B (seeds S6, S13, S18, S21, S24, and S25). Four of these six seeds produced smaller seedlings than those of the undamaged seeds (Figure 7), demonstrating that large reserve removal may reduce seedling vigor.

The absence of seeds with mechanical damage in the embryonic axis and the low number of seeds with a damaged area greater than 10% in C2 (with cracks only occurring in the scutellum and endosperm) may have been due to the maize seed structure. In addition, the embryonic axis represents a very low percentage of the seed dry matter (approximately 2%) and it is covered by the scutellum; both the shoot and root meristems are protected by the coleoptile and coleorhizae, respectively.

The average and standard deviation of the seeds and seedling parameters are summarized in Table 1. The damaged area values of 4.77 and 2.41 mm^2 in coronal planes C1 and C2 represent approximately 9% and 4% of the seed area. Thus, it was clear that mechanical damage reduced the seed mass by 46.6 mg and produced seedlings with a length and dry biomass 24% and 65% less than that of the undamaged seeds, respectively. These results support the importance of an efficient image system to evaluate mechanical damage for quality improvement of maize seeds.
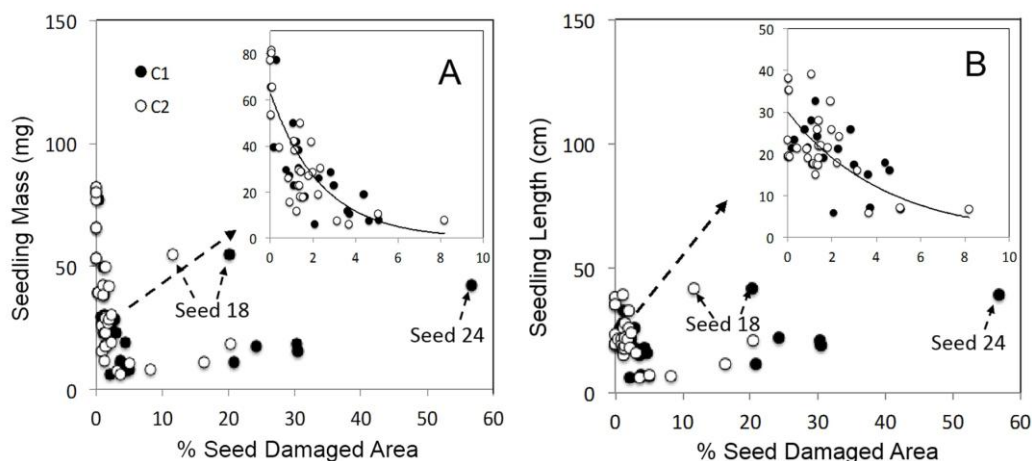

Figure 10. Correlations between the percentage of damaged area determined in micro-CT images (in the coronal C1 and C2 planes) and seedling mass (A) and length (B) for 30 maize seeds. The inserts are magnifications of the damaged areas up to 10%. Only two seeds with a damaged area greater than 10% in C1 and C2 produced a seedling length and biomass similar to that of the undamaged seeds (S18 and S24).

This research has demonstrated the applicability of the micro-CT image technique for morphological characterization of mechanically damaged maize seeds, allowing an efficient association with germination performance and seedling vigor. The technique provides a more complete and spatially resolved evaluation of internal seed morphology compared to that of the X-ray radiographic technique. However, special

attention should be paid to the acquisition parameters, pre-processing and reconstruction steps to obtain high-quality images with reduced image artifacts, high contrast and image spatial resolution and relatively low acquisition and reconstruction times.

Conclusion

The 2D transaxial, coronal and sagittal micro-CT planes provided a precise mechanical damage characterization of maize seeds, which was associated with seed germination and vigor. The increased percentage of damaged area in the coronal planes through the endosperm (C1) and endosperm + embryo (C2) was directly related to the short seedling length and lesser dry biomass. This imaging technique represents an efficient non-invasive procedure for high-resolution seed inspection and is very promising in evaluating mechanical damage, injuries caused by insects, embryonic abnormalities and other morphological alterations in seeds caused by biotic or abiotic agents.

Acknowledgements

References

Bewley, J. D., & Black, M. (1994). *Seeds:* physiology of development and germination. London, UK; Newk, US: Plenum Press.

Bino, R. J., Aartse, J. W., & Van der Burg, W. J. (1993). Non-destructive X-ray of Arabidopsis embryo mutants. *Seed Science Research*, *3*(3), 167-170. DOI: 10.1017/S0960258500001744

Boas, F. E., & Fleischmann, D. (2012). CT artifacts: causes and reduction techniques. *Imaging in Medicine*, *4*(2), 229-240.

Carvalho, M. L. M., Aelst, A. C., Eck, J. W., & Hoekstra, F. A. (1999). Pre-harvest stress cracks in maize (*Zea mays* L.) kernels as characterized by visual, X-ray and low temperature scanning electron microscopical analysis: effect on kernel quality. *Seed Science Research*, *9*(3), 227-236. DOI: 10.1017/S0960258599000239

Carvalho, M. L. M., Silva, C. D., Oliveira, L. M., Silva, D. G., & Caldeira, C. M. (2009). Teste de raios X na avaliação da qualidade de sementes de abóbora. *Revista Brasileira de Sementes*, *31*(2), 221-227. DOI: 10.1590/S0101-31222009000200026

Carvalho, N. M., & Nakagawa, J. (2012). *Sementes:* ciência, tecnologia e produção. Jaboticabal, SP: Funep.

Cicero, S. M., & Banzatto-Junior, H. L. (2003). Avaliação do relacionamento entre danos mecânicos e vigor, em sementes de milho, por meio da análise de imagens. *Revista Brasileira de Sementes*, *25*(1), 29-36. DOI: 10.1590/S0101-31222003000100006

Cicero, S. M., Heijden, G. W. A. M., Van der Burg W. J., & Bino, R. J. (1998). Evaluation of mechanical damages in seeds of maize (*Zea mays* L) by X-ray and digital imaging. *Seed Science and Technology*, *26*(3), 603-612.

Cleveland IV, T. E., Hussey, D. S., Chen, Z. Y., Jacobson, D. L., Brown, R. L., Carter-Wientjes, C., Cleveland, T. E., & Arif, M. (2008). The use of neutron tomography for the structural analysis of corn kernels. *Journal of Cereal Science*, *48*(2), 517-525. DOI: 10.1016/j.jcs.2007.12.003

Cloetens, P., Mache, R., Schlenker, M., & Lerbs-Mache, S. (2006). Quantitative phase tomography of Arabidopsis seeds reveals intercellular void network. *Proceedings of the National Academy of Sciences (USA)*, *103*(39), 14626-14630. DOI: 10.1073/pnas.0603490103

Dawson, M., Francis, J., & Carpenter, R. (2014). New views of plant fossils from Antarctica: a comparison of X-ray and neutron imaging techniques. *Journal of Paleontology*, *88*(4), 702-707. DOI: 10.1666/13-124

De Jonge, M. D., & Vogt, S. (2010). Hard X-ray fluorescence tomography - an emerging tool for structural visualization. *Current Opinion in Structural Biology*, *20*(5), 606-614. DOI: 10.1016/j.sbi.2010.09.002

Friis, E. M., Marone, F., Pedersen, K. R., Crane, P. R., & Stampanoni, M. (2014). Three-dimensional visualization of fossil flowers, fruits, seeds, and other plant remains using synchrotron radiation X-ray

tomographic microscopy (SRXTM): new insights into Cretaceous plant diversity. *Journal of Paleontology*, *88*(4), 684-701. DOI: 10.1666/13-099

Ghosh, P. K., Jayas, D. S., Gruwel, M. L. H., & White, N. D. G. (2006). Magnetic resonance image analysis to explain moisture movement during wheat drying. *Transactions of the ASABE*, *49*(4), 1181-1191. DOI: 10.13031/2013.21718

Girardin, P., Chavagnat, A., & Bockstaller, C. (1993). Determination des charactéristiques des sementes de mais grace a la radio graphie rayons X. *Seed Science and Technology*, *21*(3), 545-551.

Gomes-Junior, F. G., & Cicero, S. M. (2012). X-ray analysis to assess mechanical damage in sweet corn seeds. *Revista Brasileira de Sementes*, *34*(1), 78-85. DOI: 10.1590/S0101-31222012000100010

Milien, M., Renault-Spilmont, A. S., Cookson, S. J., Sarrazin, A., & Verdeil, J. L. (2012). Visualization of the 3D structure of the graft union of grapevine using X-ray tomography. *Scientia Horticulturae*, *144*(1), 130-140. DOI: 10.1016/j.scienta.2012.06.045

Pittia, P., Sacchetti, G., Mancini, L., Voltolini, M., Sodini, N., Tromba, G., & Zanini, F. (2011). Evaluation of microstructural properties of coffee beans by synchrotron X-ray microtomography: a methodological approach. *Journal of Food Science*, *76*(2), 222-231. DOI: 10.1111/j.1750-3841.2010.02009.x

Schneider, C. A., Rasband, W. S., & Eliceiri, K. W. (2012). NIH Image to ImageJ: 25 years of image analysis. *Nature Methods*, *9*(7), 671-675.

Staedler, Y. M., Masson, D., & Schönenberger, J. (2013). Plant tissues in 3D via X-ray tomography: simple contrasting methods allow high-resolution imaging. *PLOS ONE*, *8*(9), 1-10. DOI: 10.1371/journal.pone.0075295

Stuppy, W. H., Maisano, J. A., Colbert, M. W., Rudall, P. J., & Rowe, T. B. (2003). Three-dimensional analysis of plant structure using high-resolution X-ray computed tomography. *Trends in Plant Science*, *8*(1), 2-6.

Young, L. W., Parham, C., Zhong, Z., Chapman, D., & Reaney, M. J. T. (2007). Non-destructive diffraction enhanced imaging of seeds. *Journal of Experimental Botany*, *58*(10), 2513-2523. DOI: 10.1093/jxb/erm116